Nucleotide binding to human uncoupling protein-2 refolded from bacterial inclusion bodies

Mika B. JEKABSONS, Karim S. ECHTAY and Martin D. BRAND[1]

Medical Research Council Dunn Human Nutrition Unit, Wellcome Trust/MRC Building, Hills Road, Cambridge CB2 2XY, U.K.

Experiments were performed to test the hypothesis that recombinant human uncoupling protein-2 (UCP2) ectopically expressed in bacterial inclusion bodies binds nucleotides in a manner identical with the nucleotide-inhibited uncoupling that is observed in kidney mitochondria. For this, sarkosyl-solubilized UCP2 inclusion bodies were treated with the polyoxyethylene ether detergent $C_{12}E_9$ and hydroxyapatite. Protein recovered from hydroxyapatite chromatography was approx. 90% pure UCP2, as judged by Coomassie Blue and silver staining of polyacrylamide gels. Using fluorescence resonance energy transfer, *N*-methylanthraniloyl-tagged purine nucleoside di- and tri-phosphates exhibited enhanced fluorescence with purified UCP2. Dissociation constants determined by least-squares non-linear regression indicated that the affinity of UCP2 for these fluorescently tagged nucleotides was 3–5 μM or perhaps an order of magnitude stronger, depending on the model used. Competition experiments with [8-^{14}C]ATP demonstrated that UCP2 binds unmodified purine and pyrimidine nucleoside triphosphates with 2–5 μM affinity. Affinities for ADP and GDP were approx. 10-fold lower. These data indicate that: UCP2 (a) is at least partially refolded from sarkosyl-solubilized bacterial inclusion bodies by a two-step treatment with $C_{12}E_9$ detergent and hydroxyapatite; (b) binds purine and pyrimidine nucleoside triphosphates with low micromolar affinity; (c) binds GDP with the same affinity as GDP inhibits superoxide-stimulated uncoupling by kidney mitochondria; and (d) exhibits a different nucleotide preference than kidney mitochondria.

Key words: fluorescence resonance energy transfer (FRET), hydroxyapatite, polyoxyethylene ether detergent, UCP2.

INTRODUCTION

Uncoupling protein 1 (UCP1) retains its nucleotide binding properties when solubilized from the mitochondrial inner membrane with non-ionic detergents such as Triton X-100 [1]. In this soluble state, UCP1 can be purified by hydroxyapatite chromatography [1,2]. Under suitable conditions, UCP1 will not adsorb to hydroxyapatite, despite having 19 Glu/Asp and 28 Lys/Arg residues. Protection from hydroxyapatite is thought to occur because, when properly folded, the charged residues are shielded by both the protein's hydrophobic domains and the non-ionic detergent with which it interacts [2].

UCP2 is a mitochondrial inner membrane protein that is 59% identical with UCP1 [3]. The putative nucleotide binding domain in UCP1 is highly conserved in UCP2, suggesting that this latter protein may also bind nucleotides. Although uncoupling exhibited by yeast mitochondria expressing UCP2 is insensitive to nucleotides [4,5], recent data implicate the uncoupling in yeast as an artifactual consequence of UCP2 overexpression [5]. Support for the notion that UCP2 binds nucleotides comes from liposome reconstitution studies demonstrating that either submicromolar [6] or near-millimolar [7] purine nucleotides inhibit the measured uncoupling activity. Further studies are required to firmly establish the affinity, as well as the selectivity, of UCP2 for nucleotides. Acquiring such information is important for ultimately understanding how this protein is regulated within the cell. Towards this end, a purified, soluble UCP2 preparation would be useful for detailed nucleotide binding studies.

Although hydroxyapatite chromatography is a potential method for the purification of UCP2 solubilized from mitochondria, practical purification would be difficult because UCP2 levels are 100–1000-fold lower than those of UCP1 [8]. An alternative approach is to purify UCP2 ectopically expressed in bacterial inclusion bodies. This approach overcomes the problem of low amounts from mammalian sources, but introduces the problem of refolding the protein from a denatured state. Membrane proteins expressed in bacteria accumulate in cytoplasmic inclusion bodies that are only solubilized using denaturants such as urea or sarkosyl. Replacing the denaturant with a suitable detergent that promotes protein refolding is the main challenge. If the charged residues in native UCP2 (19 Glu/Asp; 34 Arg/Lys) are shielded as they are in UCP1, then protection from hydroxyapatite would be seen with the refolded protein. Thus our goal was to find a detergent that allowed the recovery of UCP2 from hydroxyapatite columns. We hypothesized that the use of such a method would not only select for refolded protein, but would also purify UCP2 from inclusion body contaminants. We also wanted to test the inference that UCP2 uncouples kidney mitochondria in the presence of superoxide. Thus we hypothesized that inclusion body UCP2 recovered from hydroxyapatite would exhibit nucleotide binding characteristics identical with the nucleotide-inhibited uncoupling characteristics observed previously in isolated kidney mitochondria incubated *in vitro* with the superoxide-generating system xanthine/xanthine oxidase [9].

EXPERIMENTAL

Materials

Bacterial protein extraction reagent and BCA (bicinchoninic acid) protein assay were purchased from Pierce. The polyoxyethylene ether detergents C_8E_5, $C_{12}E_9$ and $C_{13}E_{10}$ were from Sigma. $C_{10}E_6$ was from CalBiochem. Digitonin was from Fluka. Microcon and Centricon 10 kDa centrifugal filtration devices were from Millipore. Hydroxyapatite, disposable columns and

Abbreviations used: Dans, 5-(dimethylamino)naphthalene-1-sulphonyl; FRET, fluorescence resonance energy transfer; Mant, *N*-methylanthraniloyl; UCP, uncoupling protein.

[1] To whom correspondence should be addressed (e-mail martin.brand@mrc-dunn.cam.ac.uk).

silver stain were from Bio-Rad. *N*-Methylanthraniloyl (Mant)-modified nucleotides were from Molecular Probes. [8-^{14}C]ATP was from Amersham.

Preparation of UCP2 inclusion bodies

The cloning, expression and isolation of human UCP2 inclusion bodies were described in [5]. This UCP2 construct does not contain N- or C-terminal tags. The final inclusion body pellet was solubilized in 5 mM Mops, 30 mM Na_2SO_4 and 1.5 % sarkosyl, pH 7.3, for 45–60 min at 20–22 °C. Insoluble material was removed by centrifugation at 27200 ***g*** for 15 min. Solubilized inclusion bodies were stored in aliquots at −85 °C.

Detergent exchange

The simultaneous removal of sarkosyl and the addition of non-ionic detergent (C_8E_5, $C_{10}E_6$, $C_{12}E_9$, $C_{13}E_{10}$ or digitonin) was performed using centrifugal filtration devices (Microcon-10 microconcentrators). Sequential 70–90 μl aliquots of non-ionic detergent [0.1–1 % (v/v) in 5 mM Mops/30 mM Na_2SO_4, pH 7.3] were mixed with solubilized inclusion body protein (3.5 mg; 400 μl) and centrifuged at 12000 ***g*** for 5–9 min at 4 °C. This process was repeated 15 times, followed by a further 12 additions of 5 mM Mops/30 mM Na_2SO_4 until the calculated concentration of sarkosyl was 0.01 % or less (assuming simple dilution; ignoring sarkosyl being sequestered by non-ionic detergent micelles). The final sample was centrifuged at 16000 ***g*** for 30 min at 4 °C to remove insoluble material.

Hydroxyapatite chromatography

Hydroxyapatite was packed at 4 °C to approx. 16–17 ml in a 1.5 cm × 12 cm gravity-flow column using 5 mM Mops/30 mM Na_2SO_4, pH 7.3. Breakthrough fractions were collected after loading 30–40 mg of UCP2 in $C_{12}E_9$. For preliminary experiments with different detergents, 2.5–3 mg of protein was loaded on to a 2.5 ml column. Fractions containing protein were pooled and slowly concentrated over 24–25 steps to approx. 2.5 mg/ml using centrifugal filtration devices. Concentrated protein was stored in aliquots at −85 °C.

SDS/PAGE

Samples were run at 350 V for approx. 2.5 h through a 4 % (w/v) polyacrylamide stacking gel (125 mM Tris/0.1 % SDS, pH 6.8) and a 12 % (w/v) polyacrylamide resolving gel (375 mM Tris/0.1 % SDS, pH 8.8) using a running buffer consisting of 25 mM Tris, 192 mM glycine and 0.1 % SDS, pH 8.6. Gels were either stained with Coomassie Blue R-250 for 90 min in 40 % (v/v) methanol/10 % (v/v) acetic acid, or silver-stained using a commercially available kit.

Nucleotide binding measured by fluorescence resonance energy transfer (FRET)

Fluorescence ($\lambda_{ex} = 280$ nm, $\lambda_{em} = 433$ nm; slit width 1.5 nm) was measured at 10 °C in a RF-5301PC Shimadzu spectrofluorophotometer with 90 μg of hydroxyapatite-purified or 180 μg of non-purified inclusion body protein in 1 ml of 20 mM Mops/0.1 mM EDTA, pH 6.8. Titrations with Mant-modified nucleotides at concentrations from 0.01 to 60 μM were over 12 min. Competition with unmodified nucleotides (0.1–375 μM) was conducted using 1 μM Mant-ATP or Mant-GDP.

Competition experiments using [8-^{14}C]ATP

UCP2 (90 μg/ml) was incubated in 20 mM Mops/0.1 mM EDTA, pH 6.8, with 0.4 μM [8-^{14}C]ATP and 20 μM unlabelled competing nucleotide for 70 min on ice. Free [8-^{14}C]ATP was obtained by centrifuging in Microcon-10 filtration devices for 11 min at 12500 ***g*** and 4 °C. Filtrate volume (typically 150 μl from a 500 μl starting volume) was measured and [8-^{14}C]ATP content was determined by liquid scintillation counting. Association constants for competing nucleotides were calculated based on simple competition between two ligands using the following equation:

$$k_{comp} = (k_1 \cdot [L] - Y \cdot k_1 \cdot [L] - Y)/Y \cdot [\text{competing L}]$$

where k_{comp} is the association constant for competing nucleotide, k_1 is the association constant for [8-^{14}C]ATP, [L] is the free concentration of [8-^{14}C]ATP, Y is the fractional occupancy of the receptor with [8-^{14}C]ATP, and [competing L] is the concentration of competing nucleotide added. Binding constants are reported as dissociation constants, where $K_d = 1/k_{comp}$. The association constant for [8-^{14}C]ATP in the absence of competing nucleotide was calculated from a single concentration using the following equation:

$$k_1 = -Y/(Y \cdot [L] - [L])$$

Non-linear regression analysis

Equations describing ligand binding to either one or two classes of independent binding sites were written using STATA software (Stata Corporation, College Station, TX, U.S.A.), with equations as follows. For a single class of n sites:

$$n \cdot Y = (n \cdot [L]/K_d)/(1 + [L]/K_d)$$

and for two classes of n_1/n_2 sites:

$$(n_1 + n_2) \cdot Y = (n_1 \cdot [L]/K_{d1})/(1 + [L]/K_{d1}) + (n_2 \cdot [L]/K_{d2})/(1 + [L]/K_{d2})$$

where n is the number of sites, Y is the fractional occupancy, K_d is the dissociation constant, and [L] is the concentration of Mant-nucleotide. The equations were solved iteratively for n and K_d using fluorescence/maximum fluorescence data.

RESULTS

Exchanging sarkosyl for polyoxyethylene ether-type detergents using centrifugal filtration resulted in > 50 % recovery of protein in a soluble form (with a peak recovery of 80 % when using $C_{12}E_9$). In contrast, removing sarkosyl in the presence of $C_{12}E_9$ by overnight dialysis against detergent-free buffer yielded only 20 % recovery of soluble protein (results not shown). Because of the disparity in recovered soluble protein, the standard approach used for replacing sarkosyl with non-ionic detergents was centrifugal filtration.

Preliminary experiments showed that sarkosyl-solubilized UCP2 inclusion body protein was completely adsorbed by hydroxyapatite. In contrast, polyoxyethylene ether-treated UCP2 inclusion body protein was recovered in a dose- and chain-length-specific manner (Figure 1). While shorter-chain-length detergents (C_8E_5 and $C_{10}E_6$) did not provide protection from hydroxyapatite, replacing sarkosyl with $C_{12}E_9$ consistently yielded 14–18 % protein recovery (Figure 1 and Table 1). Substantially less protein was recovered using $C_{13}E_{10}$. Digitonin was ineffective over the detergent/protein ratio found to be optimal for $C_{12}E_9$ (Figure 1).

Table 1 Protein recovery after each step of the purification/refolding protocol for five independent UCP2 preparations

Sarkosyl-solubilized UCP2 inclusion body protein (starting protein) was detergent-exchanged with $C_{12}E_9$ as described in the Experimental section. Soluble protein recovered from the detergent-exchange step was applied to a hydroxyapatite column. Protein recovered in the breakthrough fractions (hydroxyapatite step) was pooled and concentrated (final protein).

	Amount of protein (mg)			
Preparation	Starting protein	Detergent exchange	Hydroxyapatite	Final protein
1	42.9	33.6	5.5	4.8
2	42.9	33.8	5.5	4.3
3	43.0	35.5	5.0	4.9
4	43.3	35.0	5.2	4.0
5	38.4	31.0	5.7	4.1
Recovery (%)	100	80	13	10

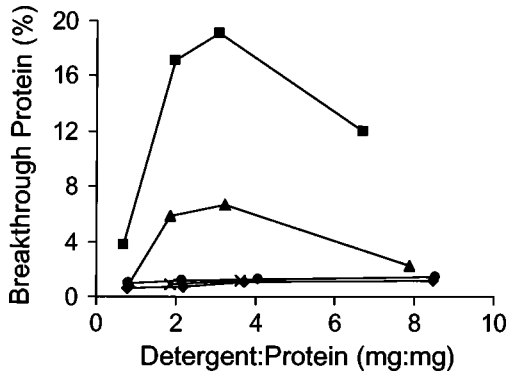

Figure 1 Hydroxyapatite chromatography of UCP2 inclusion body protein in various non-ionic detergents

Sarkosyl-solubilized UCP2 inclusion bodies were detergent-exchanged with serial additions of C_8E_5 (●), $C_{10}E_6$ (◆), $C_{12}E_9$ (■), $C_{13}E_{10}$ (▲) or digitonin (×) by centrifugal filtration. Detergent-exchanged protein was applied to a hydroxyapatite column. Breakthrough fractions were assayed for protein, and the percentage of loaded protein recovered was calculated ($n = 1$ for each detergent). The detergent/protein ratio was calculated using soluble protein recovered from the detergent exchange step, assuming 100% retention of non-ionic detergent.

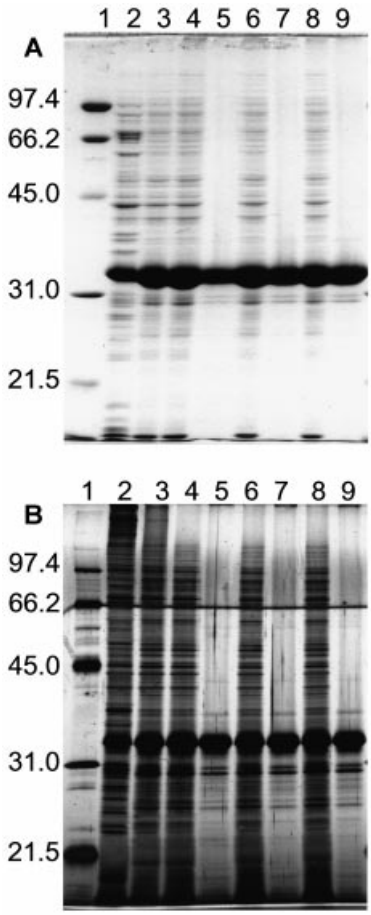

Figure 2 SDS/PAGE of inclusion body UCP2

Resolving gels (12% polyacrylamide) were electrophoresed for 140 min at 370 V and stained with either Coomassie Blue (**A**; 18 μg of protein/lane) or silver (**B**; 1 μg of protein/lane). Lanes: 1, molecular mass markers (in kDa, at left); 2, whole bacterial homogenate after induction of UCP2 for 2 h at 37 °C; 3, sarkosyl-solubilized inclusion bodies; 4/5, 6/7 and 8/9, pairs of three independent preparations showing UCP2 in $C_{12}E_9$ detergent before (lanes 4, 6 and 8) and after (lanes 5, 7 and 9) the hydroxyapatite step.

By Coomassie Blue staining, protein recovered from hydroxyapatite was predominantly UCP2 (Figure 2A). Silver staining revealed the bacterial contaminants more effectively, but still demonstrated that UCP2 recovered from hydroxyapatite was substantially purified compared with the starting inclusion body protein (Figure 2B).

Since UCPs 1, 2, and 3 bind 5-(dimethylamino)naphthalene-1-sulphonyl (Dans)-modified nucleotides [6,10], commercially available fluorescent nucleotide analogues were tested as probes to determine if hydroxyapatite-purified UCP2 assumed a nucleotide binding conformation. Fluorescence resulting from direct excitation of trinitrophenyl-ADP was unaffected by UCP2 (results not shown). A small fluorescence enhancement was observed by direct excitation of Mant-ADP in the presence of UCP2 (results not shown). Because of this, UCP2 was further tested for its ability to bind nucleotides using Mant-modified purine nucleoside di- and tri-phosphates.

When excited at 280 nm, the UCP2 emission spectrum overlapped substantially with the Mant-nucleotide excitation spectrum (Figure 3A). This overlap is one criterion necessary for measuring nucleotide binding by FRET. With 10 μM Mant-GDP, peak UCP2 emission was reduced (results not shown). This decrease is a second criterion for the use of FRET, and indicates that energy resulting from direct excitation of UCP2 was transferred to (and absorbed by) Mant-GDP rather than emitted as light. UCP2 and $C_{12}E_9$ spectra were virtually non-existent at the Mant-GDP peak emission wavelength of 440 nm (Figure 3B). Mant-GDP emission increased 4-fold and was slightly blue-shifted (peak at 433–435 nm) in the presence of UCP2 (Figure 3B). Enhanced Mant-GDP fluorescence with UCP2 compared with detergent alone is the final criterion indicating the occurrence of FRET between UCP2 and Mant-nucleotides.

An example of the fluorescent signals obtained with purified UCP2 during titrations with Mant-nucleotides is provided in Figure 4. The specificity of Mant-ATP and Mant-ADP fluorescence with purified UCP2 was tested by comparison with the signals obtained with either the completely denatured protein in sarkosyl or the protein detergent-exchanged with $C_{12}E_9$. (Figures 5A and 5B). Fluorescence with the sarkosyl-denatured protein was virtually identical with that of the $C_{12}E_9$ detergent-exchanged protein. These signals were approx. 15% of that

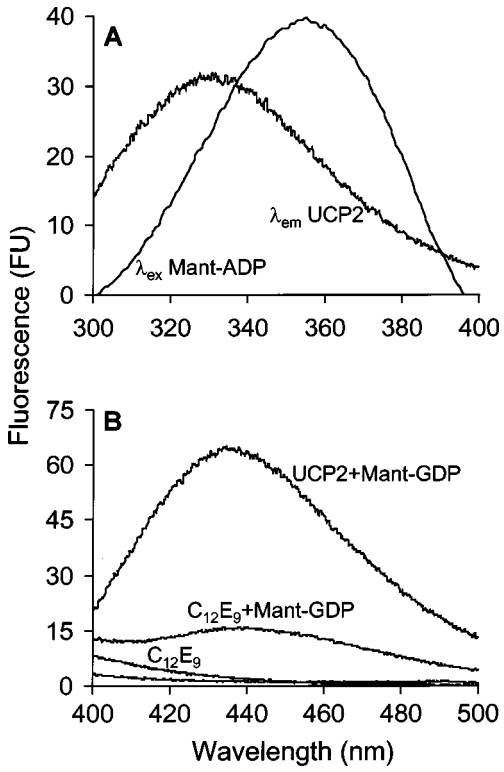

Figure 3 Fluorescence spectra of purified UCP2 and Mant-nucleotides

(**A**) The UCP2 emission spectrum (λ_{em} UCP2) was recorded with 90 μg of hydroxyapatite-purified protein/ml in 20 mM Mops/0.1 mM EDTA, pH 6.8, at 10 °C using λ_{ex} = 280 nm. The excitation spectrum of 10 μM Mant-ADP (λ_{ex} Mant-ADP) was recorded in the same buffer using λ_{em} = 445 nm. (**B**) Emission spectra (λ_{ex} = 280 nm) were recorded for Mant-nucleotide fluorescence using the same buffer as in (**A**) containing either 0.2% $C_{12}E_9$ or 90 μg/ml UCP2 (unlabelled bottom spectrum), without or with 10 μM Mant-GDP. Peak Mant-GDP fluorescence with UCP2 was at 433–435 nm. FU, fluorescence units.

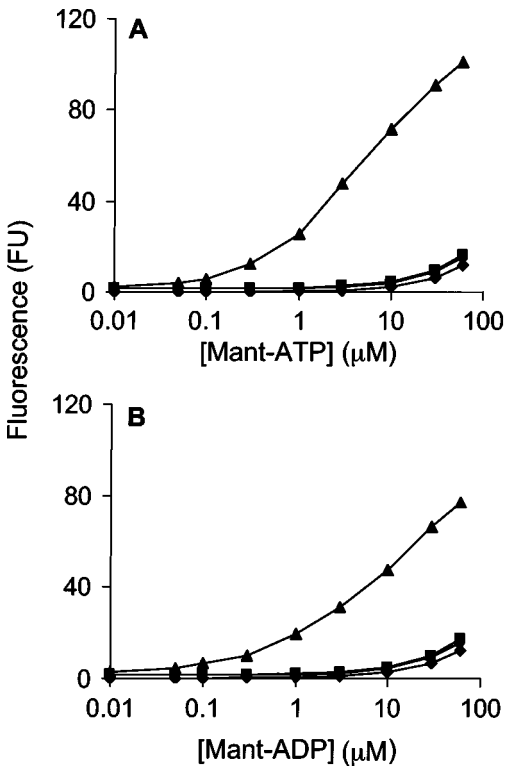

Figure 5 Mant-nucleotide fluorescence at each step of purification of inclusion body UCP2

Fluorescence (λ_{ex} = 280 nm, λ_{em} = 443 nm; slit width 1.5 nm) was recorded during titrations of either Mant-ATP (**A**) or Mant-ADP (**B**) in 20 mM Mops/0.1 mM EDTA, pH 6.8 (10 °C), containing 0.2% $C_{12}E_9$ (◆), 180 μg of sarkosyl-solubilized UCP2 inclusion body protein (■), 180 μg of detergent-exchanged $C_{12}E_9$ UCP2 inclusion body protein (●) or 90 μg of hydroxyapatite-purified UCP2 inclusion body protein (▲). Data are from a single experiment. FU, fluorescence units.

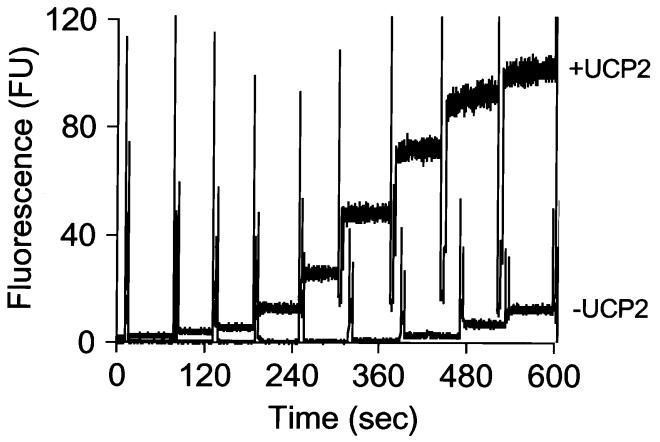

Figure 4 Representative fluorescence recordings during titrations of purified UCP2 with Mant-nucleotides

Fluorescence was recorded with (+UCP2) or without (−UCP2) 90 μg of hydroxyapaptite-purified protein/ml in 20 mM Mops/0.1 mM EDTA, pH 6.8, at 10 °C (λ_{ex} = 280 nm, λ_{em} = 433 nm; slit width 1.5 nm). Large spikes in fluorescence are points of Mant-ATP additions to final concentrations of (from left to right) 0.01, 0.05, 0.1, 0.3, 1.0, 3.0, 10, 30 and 60 μM. FU, fluorescence units.

obtained with purified UCP2. Thus the hydroxyapatite step is necessary to obtain fluorescence signals indicative of nucleotide binding.

To quantitatively describe binding of Mant-nucleotides to UCP2 by non-linear regression analysis, fluorescence signals were transformed into a form analogous to fractional occupancy data (mol of ligand bound per mol of protein). For this, fluorescence maxima were determined from double-reciprocal plots of 1/fluorescence against 1/[Mant-nucleotide]. Fluorescence/maximum fluorescence ratios were subsequently used for the analysis. When solved using a one-site binding model, dissociation constants (K_d) for UCP2 binding to Mant-nucleotides ranged from 3 to 5 μM (Table 2). This model fits the data reasonably well (Table 2). However, because the double-reciprocal plots were always non-linear (not shown) and because the pseudo-Hill plot slopes (not shown) were less than 1, more than one class of binding sites may be present; therefore the data were also analysed using a model of two classes of independent binding sites. This model (Table 2) indicated the presence of a high-affinity ($K_d \approx 0.1$ μM), low-capacity ($\approx 15\%$ of total sites) class of sites, as well as a lower-affinity ($K_d \approx 9$ μM), high-capacity ($\approx 85\%$ of total sites) class of sites.

To determine UCP2 nucleotide preference and assess the validity of the fluorescence signal reflecting binding to UCP2, we conducted competition experiments using both Mant-modified

Table 2 Non-linear regression analysis of Mant-nucleotide fluorescence data using models assuming either a single class of *n* binding sites or two independent classes of n_1 and n_2 binding sites

Data are means ± S.E.M. of three independent UCP2 preparations. UCP2 was titrated with 0.01–60 μM Mant-nucleotide. Measured fluorescence (λ_{ex} = 280 nm, λ_{em} = 433 nm) was used to calculate fluorescence maxima on double-reciprocal plots of 1/fluorescence against 1/[Mant-nucleotide]. Fluorescence/maximum fluorescence ratios (*n*; an indicator of Mant-nucleotide binding capacity) were used for non-linear regression analysis by the one- or two-site model. An asterisk (*) indicates that the value obtained from non-linear regression is not significantly different from zero.

	One-site model			Two-site model				
	n	K_d (μM)	r^2	n_1	K_{d1} (μM)	n_2	K_{d2} (μM)	r^2
Mant-ATP	0.93 ± 0.02	3.27 ± 0.34	0.992	0.30 ± 0.07	0.46 ± 0.18	0.73 ± 0.06	10.85 ± 3.01	0.997
Mant-ADP	0.91 ± 0.04	4.56 ± 0.71	0.981	0.17 ± 0.02	0.07 ± 0.03	0.87 ± 0.03	12.36 ± 1.77	0.997
Mant-GTP	0.96 ± 0.02	4.19 ± 0.36	0.994	0.08 ± 0.02	0.03 ± 0.02*	0.92 ± 0.02	6.07 ± 0.50	0.998
Mant-GDP	0.94 ± 0.03	4.52 ± 0.48	0.991	0.09 ± 0.01	0.03 ± 0.02*	0.90 ± 0.02	7.16 ± 0.63	0.998

Table 3 Selectivity of UCP2 for unmodified nucleotides by competition with Mant-GDP, Mant-ATP or [8-^{14}C]ATP

Competition data are percentage inhibition of either initial fluorescence (mean ± S.E.M.; n = 3) or binding of [8-^{14}C]ATP (mean ± S.D., n = 2) in the presence of a 50-fold excess of unlabelled nucleotide. For fluorescence studies, 90 μg of UCP2 in 1 ml was equilibrated with 1 μM Mant-nucleotide for 90 s, followed by titration with the competing nucleotide. For [8-^{14}C]ATP studies, 45 μg of UCP2 in 0.5 ml was equilibrated with 0.4 μM [8-^{14}C]ATP with or without 20 μM unlabelled nucleotide for 70 min. Dissociation constants (K_d) were calculated as described in the Experimental section. Without competing unlabelled nucleotide, the K_d values for [8-^{14}C]ATP were calculated as 2.1 and 2.5 μM for the two preparations. A lack of competition is indicated by –. Fluorescence data were analysed by one-way ANOVA. Within a column, values sharing common superscripts are not statistically different.

Competing nucleotide	Inhibition (%)			Calculated K_d for [8-^{14}C]ATP (μM)
	Mant-GDP	Mant-ATP	[8-^{14}C]ATP	
ATP	51 ± 2^{a}	32 ± 2^{a}	85 ± 6	2 ± 1
GTP	67 ± 2^{b}	52 ± 1^{b}	83 ± 7	3 ± 1
CTP	57 ± 1^{c}	44 ± 2^{c}	72 ± 1	5 ± 1
UTP	50 ± 1^{a}	29 ± 2^{a}	75 ± 3	4 ± 1
ADP	30 ± 0^{d}	15 ± 2^{d}	35 ± 7	23 ± 8
GDP	54 ± 1^{ac}	44 ± 2^{c}	39 ± 17	23 ± 16
AMP	17 ± 2^{g}	14 ± 2^{d}	−3 ± 0	–
GMP	44 ± 2^{f}	41 ± 2^{c}	−2 ± 1	–
CMP	39 ± 3^{ef}	37 ± 2^{ac}	6 ± 6	–
TMP	35 ± 5de	35 ± 3^{a}	1 ± 4	–

and radiolabelled nucleotides (Table 3). A decrease in Mant-GDP fluorescence occurred with the following potency (most to least effective): NTP > NDP > NMP (where N designates a specific purine or pyrimidine base). While these trends were also evident with Mant-ATP, the effectiveness of NTPs and NDPs to compete off the fluorescent signal was lowered (Table 3). Mant-ATP and Mant-GDP fluorescence was unaffected by titrations with Na_2SO_4 or NaCl. UCP2 consistently bound [8-^{14}C]ATP. Using a 50-fold excess of competing nucleotide, the same trend was observed as with the fluorescent nucleotides: bound [8-^{14}C]ATP was displaced by (decreasing effectiveness) NTP > NDP > NMP, with N again designating both purine and pyrimidine bases. The primary discrepancy between the radiolabelling and fluorescent data was in the ability of NMPs to decrease Mant-nucleotide fluorescence but not [8-^{14}C]ATP binding. Nonetheless, these data clearly demonstrate that UCP2 binds both purine and pyrimidine nucleotides, with a preference for triphosphate forms.

DISCUSSION

Our goal was to develop a purified UCP2 preparation and to study its nucleotide binding properties. We found that purification of UCP2 from inclusion bodies can be achieved using the same principle as for purification of UCP1 from brown adipose tissue [1,2] – by protection from adsorption to hydroxyapatite. Our finding that $C_{12}E_9$ is optimal for UCP2 purification is consistent with the work of Schroers et al. [11], who found that $C_{12}E_8$ was optimal for the recovery of soluble inclusion body phosphate carrier (15% identical with UCP2) after dialysis. Thus mitochondrial anion carrier family proteins expressed in bacteria may in general prefer medium-chain-length polyoxyethylene ether-type detergents as an environment that is conducive for refolding. It is important to note that, once treated with $C_{12}E_9$ detergent, the majority of UCP2 (approx. 70%) does adsorb to hydroxyapatite, while a smaller population (approx. 30%) does not (based on the starting inclusion body protein being 50% pure [5] and the hydroxyapatite-recovered protein being 90% pure). Since sarkosyl-denatured UCP2 adsorbs completely to hydroxyapatite, we infer that $C_{12}E_9$-exchanged UCP2 that adsorbs to this matrix is denatured. Conversely, we suspect that the protected UCP2 has assumed a refolded conformation. This refolded state apparently results in many of the 53 Glu/Asp/Lys/Arg residues within the protein being shielded from the positive and negative charges of the hydroxyapatite matrix.

The uncoupling that is observed in liposomes containing inclusion body UCP2 or UCP3 is inhibited by purine nucleotides [6,7]. Additionally, superoxide-stimulated uncoupling via UCP3 in mouse skeletal muscle is inhibited by purine nucleotides [9]. Therefore nucleotide binding is one method of determining if hydroxyapatite-purified UCP2 assumes a refolded conformation. It is important to emphasize that protein refolding can occur to different degrees. For example, under any given set of *in vitro* conditions, certain secondary structure domains within a protein may interact to give a partial tertiary structure, while other domains may not order correctly. While the recovery of nucleotide binding would indicate the refolding of the domain involved, it does not necessarily indicate refolding of the entire protein to its *in vivo* state. Thus our reference to refolded UCP2 should only be taken as the recovery of a functional nucleotide binding domain, and not necessarily as an indication that UCP2 has assumed a completely native state.

Using FRET methods, Mant-modified nucleotides exhibited enhanced fluorescence with purified UCP2 compared with the non-purified inclusion body protein. Because FRET efficiency requires a close association between protein and fluorescent

ligand, these data suggest that UCP2 binds nucleotides. To our surprise, non-purified, $C_{12}E_9$-exchanged UCP2 did not exhibit enhanced fluorescence with Mant-ATP or Mant-ADP compared with the sarkosyl-denatured inclusion body protein (Figure 5). Thus the $C_{12}E_9$ detergent-exchange step is sufficient for protecting approx. 30% of UCP2 from hydroxyapatite adsorption, but is insufficient for the protein to achieve a nucleotide binding conformation. We hypothesize that hydroxyapatite removes an inhibitory factor which prevents nucleotide binding to UCP2. The inhibitory factor may either be residual bound sarkosyl that is sufficient to prevent formation of the nucleotide binding domain but insufficient to expose the charged residues to the hydroxyapatite matrix, or a contaminating bacterial protein that interferes with UCP2. In either case, these data support our hypothesis that hydroxyapatite can be used to select for refolded inclusion body UCP2.

In the absence of Mg^{2+}, UCP1 binds purine nucleoside di- and tri-phosphates with 1–5 μM affinity at pH 6.7 [2,12]. Assuming a single class of binding sites, we found that UCP2 bound Mant-modified purine nucleoside di- and tri-phosphates with 3–5 μM affinity at pH 6.8 (Table 2). Analysis by a two-site model yielded binding constants significantly different from zero with titrations of Mant-ATP and -ADP, but not with titrations of Mant-GTP and -GDP (Table 2). Thus we cannot unequivocally state that Mant-modified nucleotides associate with a single class of receptor sites in this UCP2 preparation. Although further work is required to resolve this issue, these data indicate that UCP2 binds Mant-nucleoside di- and tri-phosphates with an affinity similar to or greater than that of soluble UCP1 for unmodified purine nucleotides.

UCP1 preferentially binds purine nucleotides; however, both purine and pyrimidine nucleoside di- and tri-phosphates induce respiratory control and compete for GDP binding sites in brown adipose tissue mitochondria [13,14]. To determine the nucleotide preference and affinity of UCP2, we assessed the ability of unmodified nucleotides to compete with both bound [8-^{14}C]ATP and Mant-GDP or Mant-ATP fluorescence. Because radiolabelled nucleotides are minimally modified and reliably counted, competition with [8-^{14}C]ATP is likely to reflect the true UCP2 nucleotide selectivity. Our finding that UCP2 prefers purine nucleoside triphosphates over diphosphates at pH 6.8 agrees with the K_I values reported for inclusion body UCP2 reconstituted into liposomes [6]. However, quantitatively we found that UCP2 strongly prefers the triphosphate over diphosphate moieties, by approx. 10-fold, compared with a 2-fold preference reported by Echtay et al. [6]. By comparison, UCP1 exhibits a weaker triphosphate preference at pH 6.8 [2,6,12]. Our additional finding that UCP2 binds pyrimidine nucleoside triphosphates almost as well as their purine counterparts contrasts with the apparent weaker affinity of UCP1 for pyrimidine nucleotides [13,14].

Echtay et al. [9] inferred that exogenously produced superoxide uncouples kidney mitochondria via UCP2. We hypothesized that the GDP inhibition constant and nucleotide selectivity in kidney mitochondria would be identical with those measured with inclusion body UCP2. However, our data do not conclusively support this hypothesis. The 17 μM inhibition constant reported for GDP in kidney mitochondria [9] agrees well with our current estimate of 23 μM using competition experiments with purified UCP2. However, the present experiments show that pyrimidine nucleoside triphosphates are much stronger ligands with purified UCP2 than with kidney mitochondria. This discrepancy indicates either that refolded UCP2 does not assume a completely native conformation (as discussed above), or that human UCP2 has a different nucleotide preference from that of rat UCP2. Species differences in the nucleotide preference of UCP1 have been noted [15,16]. A third possibility, which we consider less likely, is that superoxide does not uncouple kidney mitochondria through effects on UCP2.

Nucleoside monophosphates did not compete with [8-^{14}C]ATP binding. In contrast, these nucleotides did reduce the fluorescence signal of 1 μM Mant-GDP and Mant-ATP. This discrepancy is unlikely to be due to the higher concentrations of competing nucleotide (2.5-fold) used with the Mant-nucleotides. In both sets of experiments the amount of competing nucleotide was kept constant at a 50-fold excess. The decrease in fluorescence is more likely to be related to a non-specific quenching effect rather than to true competition.

The fact that UCP2 apparently binds Mant-ADP and Mant-GDP as effectively as the Mant-modified nucleoside triphosphates (Table 2) does not necessarily contradict our earlier conclusion that UCP2 binds unmodified nucleoside diphosphates less strongly than the corresponding triphosphates (Table 3). Huang and Klingenberg [10] have shown that UCP1 binds 5-(dimethylamino)naphthalene-1-carbonyl (Dan)- and Dans-modified purine nucleoside monophosphates as well as the modified triphosphates, despite the fact that unmodified monophosphates have K_d values that are approx. 100-fold greater than those of unmodified triphosphates. Moreover, UCP1 binds Dans-modified purine nucleoside di- and tri-phosphates with higher affinity than their unmodified counterparts. By analogy, modification by Mant may produce a ligand that effectively overcomes the selectivity of UCP2 for the different phosphate forms. The hydrophobic Mant group could cause a pronounced hydrophobic interaction with UCP2 that renders the phosphate–protein interaction less important.

In summary, we report a method for the purification and at least partial refolding of bacterially expressed human UCP2. Sarkosyl-solubilized inclusion body UCP2 assumes a nucleotide binding conformation when treated with $C_{12}E_9$ detergent and hydroxyapatite. At pH 6.8, purine and pyrimidine nucleoside triphosphates are the primary ligands for UCP2. FRET occurs between UCP2 and Mant-modified nucleotides, indicating that these probes may be useful in monitoring nucleotide binding to the purified protein. Further studies are required to determine the utility of Mant-nucleotides for monitoring nucleotide binding to UCP2, and to establish the binding constants for nucleotides at physiological ionic strength, temperature and pH.

This work was supported by a grant from Knoll Pharmaceuticals, Nottingham, U.K. We thank Athel Cornish-Bowden for helpful comments with non-linear regression analysis.

REFERENCES

1 Lin, C. S. and Klingenberg, M. (1980) Isolation of the uncoupling protein from brown adipose tissue mitochondria. FEBS Lett. **113**, 299–303
2 Lin, C. S. and Klingenberg, M. (1982) Characteristics of the isolated purine nucleotide binding protein from brown fat mitochondria. Biochemistry **21**, 2950–2956
3 Fleury, C., Neverova, M., Collins, S., Raimbault, S., Champigny, O., Levi-Meyrueis, C., Bouillaud, F., Seldin, M. F., Surwit, R. S., Ricquier, D. and Warden, C. H. (1997) Uncoupling protein-2: a novel gene linked to obesity and hyperinsulinemia. Nat. Genet. **15**, 269–272
4 Rial, E., Gonzalez-Barroso, M., Fleury, C., Iturrizaga, S., Sanchis, D., Jimenez-Jimenez, J., Ricquier, D., Goubern, M. and Bouillaud, F. (1999) Retinoids activate proton transport by the uncoupling proteins UCP1 and UCP2. EMBO J. **18**, 5827–5833
5 Stuart, J. A., Harper, J. A., Brindle, K. M., Jekabsons, M. B. and Brand, M. D. (2001) Physiological levels of mammalian uncoupling protein 2 do not uncouple yeast mitochondria. J. Biol. Chem. **276**, 18633–18639
6 Echtay, K. S., Winkler, E., Frischmuth, K. and Klingenberg, M. (2001) Uncoupling proteins 2 and 3 are highly active H^+ transporters and highly nucleotide sensitive when activated by coenzyme Q (ubiquinone). Proc. Natl. Acad. Sci. U.S.A. **98**, 1416–1421

7 Jaburek, M., Varecha, M., Gimeno, R. E., Dembski, M., Jezek, P., Zhang, M., Burn, P., Tartaglia, L. A. and Garlid, K. D. (1999) Transport function and regulation of mitochondrial uncoupling proteins 2 and 3. J. Biol. Chem. **274**, 26003–26007
8 Pecqueur, C., Alves-Guerra, M. C., Gelly, C., Levi-Meyrueis, C., Couplan, E., Collins, S., Ricquier, D., Bouillaud, F. and Miroux, B. (2001) Uncoupling protein 2: in vivo distribution, induction upon oxidative stress, and evidence for translational regulation. J. Biol. Chem. **276**, 8705–8712
9 Echtay, K. S., Roussel, D., St-Pierre, J., Jekabsons, M. B., Cadenas, S., Stuart, J. A., Harper, J. A., Roebuck, S. J., Morrison, A., Pickering, S. et al. (2002) Superoxide activates mitochondrial uncoupling proteins. Nature (London) **415**, 96–99
10 Huang, S. G. and Klingenberg, M. (1995) Fluorescent nucleotide derivatives as specific probes for the uncoupling protein: thermodynamics and kinetics of binding and the control by pH. Biochemistry **34**, 349–360
11 Schroers, A., Burkovski, A., Wohlrab, H. and Kramer, R. (1998) The phosphate carrier from yeast mitochondria. Dimerization is a prerequisite for function. J. Biol. Chem. **273**, 14269–14276
12 Klingenberg, M. (1988) Nucleotide binding to uncoupling protein. Mechanism of control by protonation. Biochemistry **27**, 781–791
13 Heaton, G. M. and Nicholls, D. G. (1977) The structural specificity of the nucleotide-binding site and the reversible nature of the inhibition of proton conductance induced by bound nucleotides in brown-adipose-tissue mitochondria. Biochem. Soc. Trans. **5**, 210–212
14 Pedersen, J. I. (1970) Coupled endogenous respiration in brown adipose tissue mitochondria. Eur. J. Biochem. **16**, 12–18
15 Flatmark, T. and Pedersen, J. I. (1975) Brown adipose tissue mitochondria. Biochim. Biophys. Acta **416**, 53–103
16 Nicholls, D. G. (1979) Brown adipose tissue mitochondria. Biochim. Biophys. Acta **549**, 1–29

Received 25 March 2002/13 May 2002; accepted 27 May 2002
Published as BJ Immediate Publication 27 May 2002, DOI 10.1042/BJ20020469